Parameterizing both path amplitude and delay variations of underwater acoustic channels for block decoding of orthogonal frequency division multiplexing

Xiaoka Xu, Zhaohui Wang, Shengli Zhou,[a] and Lei Wan
Department of Electrical and Computer Engineering, University of Connecticut, 371 Fairfield Road, Unit 2157, Storrs, Connecticut 06269

(Received 11 October 2011; revised 28 March 2012; accepted 2 April 2012)

There are no commonly-agreed mathematical models for the input–output relationship of underwater acoustic channels. For each path in a time-varying multipath channel within a short period of time (e.g., one short data block), this paper proposes to use one polynomial to approximate the amplitude variation and another polynomial up to the first order to approximate the delay variation within a block duration. Under such a channel parameterization, the discrete-time channel input–output relationship tailored to zero-padded orthogonal-frequency-division-multiplexing (OFDM) transmissions is then derived, based on which an OFDM receiver is validated using experimental data collected during the 2008 Surface Processes and Acoustic Communications Experiment. For channels with a short coherence time, the numerical results show that incorporating both the amplitude and delay variations improves the system performance. © *2012 Acoustical Society of America*. [http://dx.doi.org/10.1121/1.4707460]

PACS number(s): 43.60.Dh, 43.60.Uv, 43.60.Ek [ZHM] Pages: 4672–4679

I. INTRODUCTION

The underwater acoustic (UWA) channel is generally recognized as one of the most difficult communication channels today.[1,2] It has long delay spreads (on the order of 10–100 ms) and fast spatial/temporal variations. Being both time- and frequency-selective, a UWA channel introduces significant inter-symbol-interference (ISI) in single-carrier transmissions[3,4] and inter-carrier-interference (ICI) in multicarrier transmissions,[5,6] especially for high-data-rate communications.

A proper description of the channel input–output relationship is often essential to an effective receiver design. For wireless radio communications, a tap-based channel model is the primary choice to characterize the channel impulse response (CIR) for time-invariant frequency-selective channels, where the amplitudes of the channel taps are drawn from a statistical distribution, such as the Rayleigh, Rican, or Nakagami distribution.[7] For block transmissions over time-varying channels, there are several options available such as the basis expansion model (BEM) model,[8–10] the radial basis function (RBF) model,[11,12] and the polynomial amplitude-variation channel model.[13,14] All of these models assume that the tap or path delays are static within a short block duration. This assumption is often suitable for wireless radio channels, but may not be for most UWA channels.

In UWA related applications, channel modeling often refers to modeling the physical propagation effects; for example, the Ray-based acoustic scattering approach[15] and the Parabolic Equation (PE) based approach.[16,17] From a signal processing point of view, several different mathematical descriptions of the channel input–output relationship have been used in different receiver designs. For single carrier transmissions, it is common to assume that the frequency-selective channel is varying slowly from symbol to symbol, and hence adaptive channel equalization or estimation is needed.[3,4,18] For block transmissions, the following approaches have been adopted.

(1) *Quasi-static multipath channel*. After main Doppler mitigation through resampling and carrier-frequency-offset (CFO) compensation, the multipath channel can be assumed to be time-invariant. This is frequently used for multicarrier systems[19–22] and single-carrier block transmissions with frequency-domain equalization.[23,24]
(2) *BEM*. The BEMs for time-varying radio channels have been tested in UWA communications.[25–28]
(3) *Delay variation parameterization.* For multicarrier receiver designs,[5,29] it is assumed that the amplitude of each path in a multipath channel is nearly constant, while the delay variation is approximately linear with time within each orthogonal-frequency-division-multiplexing (OFDM) block duration. For a multipath channel with a number of paths, its impulse response is parameterized by a number of (amplitude, delay, Doppler scale) triplets.

This paper proposes to parameterize both amplitude and delay variations for a time-varying multipath channel. In particular, one polynomial is used to approximate the amplitude variation and another polynomial up to the first order is used to approximate the delay variation for each path within block duration. Under such a parameterization, an exact discrete-time channel input–output relationship tailored to zero-padded (ZP) OFDM is derived. An OFDM receiver for an existing signal design in our prior work[28,29] is then specified, which uses the orthogonal matching pursuit (OMP) algorithm to estimate the channel parameters. Data sets collected in the 2008 Surface Processes and Acoustic

[a]Author to whom correspondence should be addressed. Electronic mail: shengli@engr.uconn.edu

 0001-4966/2012/131(6)/4672/8/$30.00

Communications Experiment (SPACE08) experiment are used to validate the benefits of parameterization of both path amplitude and delay variations.

When the channels are slowly-varying, the performance of the receivers assuming different polynomial orders is similar to each other. When the channels are quickly-varying, it is shown that using high-order polynomials can help to improve the system performance. For the tested SPACE08 data sets, a second-order fitting on the amplitude variation with a zeroth-order fitting on the delay variation leads to a similar performance with the currently used approach with zeroth-order amplitude and first-order delay fittings,[28] while a first-order fitting on both amplitude and delay variations renders better performance.

The rest of this paper is organized as follows. The multipath channel with polynomial approximations on the path amplitude and delay variations is presented in Sec. II. Section III derives the discrete-time channel input–output relationship for ZP-OFDM. Verification with experimental data is provided in Sec. IV. Section V contains the conclusions.

II. PARAMETERIZING PATH AMPLITUDE AND DELAY VARIATIONS

A time-varying multipath channel which consists of N_{pa} discrete paths can be expressed as

$$h(t,\tau)=\sum_{p=1}^{N_{\text{pa}}}\mathcal{A}_p(t)\delta(\tau-\tau_p(t)), \tag{1}$$

where $\mathcal{A}_p(t)$ and $\tau_p(t)$ are the amplitude and delay of the pth path, respectively. Due to the motion of the transmitter and the receiver as well as the medium variability, both the amplitudes and the delays are time-varying. Let $\tilde{x}(t)$ denote the transmitted signal in the passband, and $\tilde{y}(t)$ the received signal in the passband. The channel input–output relationship is

$$\begin{aligned}\tilde{y}(t)&=\tilde{x}(t)\star h(t,\tau)+\tilde{w}(t)\\&=\int_0^{\tau_{\max}}\tilde{x}(t-\tau)h(t-\tau,\tau)d\tau+\tilde{w}(t)\\&=\sum_{p=1}^{N_{\text{pa}}}\mathcal{A}_p(t-\tau_p(t))\tilde{x}(t-\tau_p(t))+\tilde{w}(t),\end{aligned} \tag{2}$$

where $\tau_{\max}$ is the maximum delay and $\tilde{w}(t)$ is the additive noise.

Within one block of duration T_{bl}, e.g., one OFDM symbol, we adopt the following two approximations on each individual path.

(1) The amplitude variation within one block can be approximated by a polynomial up to order N_{amp}

$$\begin{aligned}\mathcal{A}_p(t)&\approx A_p^{(0)}-A_p^{(1)}t+\frac{1}{2}A_p^{(2)}t^2+\cdots\\&\quad+\frac{(-1)^{N_{\text{amp}}}}{N_{\text{amp}}!}A_p^{(N_{\text{amp}})}t^{N_{\text{amp}}}\\&=\sum_{n=0}^{N_{\text{amp}}}\frac{(-1)^n}{n!}A_p^{(n)}t^n,\quad t\in[0,T_{\text{bl}}].\end{aligned} \tag{3}$$

(2) The delay variation within one block can be approximated by a first-order polynomial

$$\tau_p(t)\approx\tau_p-a_pt,\quad t\in[0,T_{\text{bl}}], \tag{4}$$

where τ_p is the initial delay and a_p is first-order derivative of $\tau_p(t)$. (The parameter a_p is often termed as the Doppler scaling factor.) The zeroth-order approximation is obtained by setting $a_p=0,\forall p$.

The approximations in Eqs. (3) and (4) are basically the Taylor expansions of $\mathcal{A}_p(t)$ and $\tau_p(t)$ within one block duration, truncated to the N_{amp}th order on the amplitude and to the first order on the delay, respectively. With such approximations, the multipath channel in Eq. (1) is simplified as

$$h(t,\tau)\approx\sum_{p=1}^{N_{\text{pa}}}\left(\sum_{n=0}^{N_{\text{amp}}}\frac{(-1)^n}{n!}A_p^{(n)}t^n\right)\delta(\tau-(\tau_p-a_pt)), \tag{5}$$

and the received passband signal in Eq. (2) is simplified as

$$\begin{aligned}\tilde{y}(t)\approx&\sum_{p=1}^{N_{\text{pa}}}\sum_{n=0}^{N_{\text{amp}}}\frac{(-1)^n}{n!}A_p^{(n)}\big((1+a_p)t-\tau_p\big)^n\\&\times\tilde{x}\big((1+a_p)t-\tau_p\big)+\tilde{w}(t).\end{aligned} \tag{6}$$

Some special cases of Eqs. (5) and (6) have been studied in the literature.

(1) If $N_{\text{amp}}=0$ and $a_p=0,\forall p$, the multipath channel in Eq. (5) is time-invariant. This is rarely the case in underwater environments. However, after proper Doppler compensation, the equivalent channel may be viewed as approximately time-invariant.[19,20]
(2) If $N_{\text{amp}}=0$ and there exists at least one path with $a_p\neq0$, the multipath channel in Eq. (5) characterizes the delay variation through a first-order approximation but assumes the path amplitude nearly constant.[5,29]
(3) If $N_{\text{amp}}>0$ and $a_p=0,\forall p$, the multipath channel in Eq. (5) is in agreement with the polynomial amplitude-variation channel model used for wireless radio channels.[13,14] In this case, the delays are assumed static but the amplitudes are time-varying.

A. Remark 1

During the course of this work, we have also pursued a high-order polynomial approximation on the delay as

$$\begin{aligned}\tau_p(t)\approx&a_p^{(0)}-a_p^{(1)}t+\frac{1}{2}a_p^{(2)}t^2+\cdots\\&+\frac{(-1)N_{\text{delay}}}{N_{\text{delay}}!}a_p^{(N_{\text{delay}})}t^{N_{\text{delay}}}.\end{aligned} \tag{7}$$

We have obtained the closed-form expressions of the received OFDM signals using known $\text{erfc}(\cdot)$ functions for $N_{\text{delay}}=2$. However, the expressions are somewhat complicated; hence their use in practical receiver designs seems limited. Hence, this paper only includes the delay approximation up to the first-order polynomial fitting.

B. Remark 2

The expressions in Eqs. (5) and (6) capture the channel effect from a pure signal processing perspective, i.e., they parameterize how the output signal shall be related to the input signal subject to fitting errors. One physical propagation path may be approximated by several candidate paths in Eq. (5) due to scattering, distortion, and timing resolution issues. Or, several physical paths may be approximated by one candidate path in Eq. (5) when the physical paths cannot be resolved due to the limited signal bandwidth.

III. ZP-OFDM SYSTEM MODEL

Using zero-padded OFDM as the signaling format to explore the usefulness of the channel parameterization in Eq. (5), we next derive a discrete-time matrix-vector representation of the channel input–output relationship. This representation will be used in the signal design and receiver algorithms specified in Sec. IV.

A. Transmitted signal

Let T denote the signal duration and T_g the zero padding interval. The OFDM block duration is $T_{\text{bl}} = T + T_g$. The kth subcarrier is at frequency

$$f_k = f_c + k/T, \quad k = -K/2, \ldots, K/2 - 1, \tag{8}$$

where f_c is the carrier frequency and K subcarriers are used so that the bandwidth is $B = K/T$. Let $s[k]$ denote the information symbol to be transmitted on the kth subcarrier and $\mathcal{S}_{\text{all}} = \{-K/2, \ldots, K/2 - 1\}$ the set of all subcarriers.

The transmitted signal in the passband is given by

$$\tilde{x}(t) = 2\text{Re}\left\{\left[\sum_{k\in\mathcal{S}_{\text{all}}} s[k]e^{j2\pi(k/T)t}g(t)\right]e^{j2\pi f_c t}\right\}, \quad t \in [0, T_{\text{bl}}], \tag{9}$$

where $g(t)$ is a pulse-shaping window with its Fourier transform $G(f)$. The Fourier transform of $\tilde{x}(t)$ at the positive frequency is

$$\tilde{X}(f) = \sum_{k\in\mathcal{S}_{\text{all}}} s[k]G(f - f_k), \quad \forall f > 0. \tag{10}$$

For a rectangular window

$$g(t) = \begin{cases} 1/T, & t \in [0, T] \\ 0, & \text{otherwise}, \end{cases} \tag{11}$$

its Fourier transform is

$$G(f) = \frac{\sin(\pi f T)}{\pi f T} e^{-j\pi f T}. \tag{12}$$

Other pulse shapers, such as raised cosine window, can be applied as well.

B. Received signal

With $\tilde{x}(t)$ in Eq. (9), the Fourier transform of $\tilde{y}(t)$ [cf. Eq. (6)] in the positive frequency range is

$$\tilde{Y}(f) = \sum_{p=1}^{N_{\text{pa}}}\sum_{n=0}^{N_{\text{amp}}} \frac{(-1)^n}{n!}\frac{A_p^{(n)}}{1+a_p}\left(\frac{j}{2\pi}\right)^n e^{-j2\pi[f/(1+a_p)]\tau_p} \times \sum_{k\in\mathcal{S}_A} s[k]G^{(n)}\left(\frac{f}{1+a_p} - f_k\right) + \tilde{W}(f), \tag{13}$$

where $\tilde{W}(f)$ is the Fourier transform of $\tilde{w}(t)$, and the derivatives on $G(f)$ are defined as

$$G^{(n)}(f) = \frac{d^n G(f)}{df^n}. \tag{14}$$

The receiver performs the following three steps to obtain the frequency-domain samples from the passband signal.[19]

(1) The received signal $\tilde{y}(t)$ is resampled with a resampling factor $\hat{a}$, leading to $\tilde{z}(t) = \tilde{y}(t/(1+\hat{a}))$, where $\hat{a}$ could be estimated by a preamble preceding data transmission.[30]
(2) The passband signal $\tilde{z}(t)$ is shifted to baseband $z(t) = \text{LPF}\ (\tilde{z}(t)e^{-j2\pi f_c t})$, where LPF$(\cdot)$ stands for low-pass filtering. Fine Doppler shift compensation is performed on the baseband signal to obtain $z(t)e^{-j2\pi\hat{\epsilon}t}$, where $\hat{\epsilon}$ is the estimated residual mean Doppler shift. One way of obtaining $\hat{\epsilon}$ is to minimize the energy on the null subcarriers.[19]
(3) The sample on the mth subcarrier is obtained as

$$z[m] = \int_0^{T_{\text{bl}}} z(t)e^{-j2\pi\hat{\epsilon}t}e^{-j2\pi(m/T)t}dt. \tag{15}$$

The samples on all the subcarriers are obtained simultaneously by fast Fourier transform (FFT) operation.

It can be easily verified that

$$z[m] = Z(m/T + \hat{\epsilon}) = \tilde{Z}(f_m + \hat{\epsilon}) = (1+\hat{a})\tilde{Y}((1+\hat{a})(f_m + \hat{\epsilon})), \tag{16}$$

where $Z(f)$ is the spectrum of $z(t)$, and $\tilde{Z}(f)$ is the spectrum of $\tilde{z}(t)$. Using the expression in Eq. (13), we obtain

$$z[m] = \sum_{k\in\mathcal{S}_A} s[k]\underbrace{\sum_{p=1}^{N_{\text{pa}}} e^{-j2\pi(m/T)\tau'_p}\left\{\sum_{n=0}^{N_{\text{amp}}}\frac{(-1)^n}{n!}\frac{A_p^{(n)}e^{-j2\pi(fc+\hat{\epsilon})\tau'_p}}{1+b_p}\left(\frac{j}{2\pi}\right)^n G^{(n)}(\beta_{m,k}(b_p))\right\}}_{H(m,k)} + v[m], \tag{17}$$

where $v[m]$ is a noise sample,

$$b_p = \frac{a_p - \hat{a}}{1 + \hat{a}} \tag{18}$$

is the residual Doppler scaling factor after resampling,

$$\tau'_p = \frac{\tau_p}{1 + b_p} \tag{19}$$

is the scaled delay after resampling, and

$$\beta_{m,k}(b_p) = \frac{m-k}{T} + \frac{\hat{\epsilon} - b_p f_m}{1 + b_p}. \tag{20}$$

Stack the transmitted symbols and frequency measurements at all subcarriers into vectors $\mathbf{s} := [s[-K/2], \ldots, s[K/2-1]]^T$ and $\mathbf{z} := [z[-K/2], \ldots, z[K/2-1]]^T$, respectively. For each index p, define a variable

$$\xi_p^{(n)} = \frac{(-1)^n}{n!} \left(\frac{j}{2\pi}\right)^n \frac{A_p^{(n)}}{1 + b_p} e^{-j2\pi(f_c + \hat{\epsilon})\tau'_p}, \tag{21}$$

a diagonal matrix with element

$$[\mathbf{\Lambda}_p]_{m,m} = e^{-j2\pi(m/T)\tau'_p}, \tag{22}$$

and a $K \times K$ matrix with element

$$[\mathbf{\Gamma}_p^{(n)}]_{m,k} = G^{(n)}(\beta_{m,k}(b_p)). \tag{23}$$

The matrix-vector based input–output relationship is thus

$$\mathbf{z} = \mathbf{H}\mathbf{s} + \mathbf{v}, \tag{24}$$

where $\mathbf{v}$ contains the additive noise and the channel mixing matrix can be expressed as

$$\mathbf{H} = \sum_{p=1}^{N_{\text{pa}}} \sum_{n=0}^{N_{\text{amp}}} \xi_p^{(n)} \mathbf{\Lambda}_p \mathbf{\Gamma}_p^{(n)}. \tag{25}$$

[The expression of $H[m, k]$, the element of $\mathbf{H}$, is also defined in Eq. (17).] Although $\mathbf{H}$ in Eq. (25) has K^2 entries, it is characterized by N_{pa} sets of parameters $(A_p^{(0)}, \ldots, A_p^{(N_{\text{amp}})}, \tau'_p, b_p)$.

Equation (24) provides a discrete-time channel input–output relationship for a generic ZP-OFDM transmission in the presence of the multipath channel in Eq. (5). This formulation includes the derivations in existing works[5,19] as special cases.

IV. EXPERIMENTAL VALIDATION

In our prior work,[28,29] we carried out comparisons between the multipath channel with delay variation parameterization with the BEM channel model, and showed that the former leads to better performance than the latter. Hence, we will use the multipath channel with delay variation parameterization as the benchmark, and use the same signal design and the experimental data sets[28] to validate the proposed parameterization in Eq. (5).

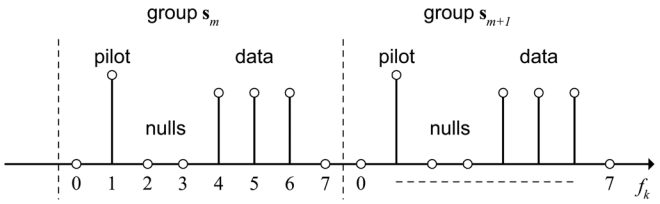

FIG. 1. Subcarrier allocation.

A. Signal design

The system bandwidth is $B = 9.76$ kHz with a center frequency of $f_c = 13\,000$ Hz. A total of $K = 1024$ subcarriers are used, and hence the subcarrier spacing is $B/K = 9.54$ Hz and the symbol duration is $T = K/B = 104.88$ ms. The guard time is chosen as $T_g = 24.6$ ms, leading to an OFDM block duration $T_{\text{bl}} = T + T_g = 129.48$ ms.

To decouple channel estimation from data demodulation at the receiver, the subcarriers are carefully arranged, as shown in Fig. 1. Specifically, define an 8×1 subvector $\mathbf{s}_m$ that contains one pilot symbol, p_m, and three data symbols, $\mathbf{d}_m = [d_{m,1}, d_{m,2}, d_{m,3}]^T$ in the following way:

$$\mathbf{s}_m = [0 \quad p_m \quad \mathbf{0}_{1\times 2} \quad \mathbf{d}_m^T \quad 0]^T. \tag{26}$$

On each OFDM block, the symbol vector $\mathbf{s}$ consists of $K/8$ subvectors so that

$$\mathbf{s} = [\mathbf{s}_{-K/16}^T, \ldots, \mathbf{s}_{K/16-1}^T]^T. \tag{27}$$

Hence, there are $N_p = 128$ pilot subcarriers regularly spaced. Some data subcarriers at the edge of the frequency band are turned off, with only $N_d = 336$ data subcarriers in the middle groups used for data delivery. With a constellation of size M and rate 1/2 nonbinary LDPC coding,[31] the spectrum efficiency is

$$\alpha = \frac{T}{T + T_g} \cdot \frac{336}{1024} \cdot \frac{1}{2} \cdot \log_2 M. \tag{28}$$

With 16-QAM constellation, the spectrum efficiency is 0.53 bits/s/Hz and the data rate is 5.19 kb/s.

B. Receiver implementation

To have low-complexity processing, the receiver adopts an assumption that the ICI beyond the direct neighbors can be ignored,[28,29] i.e., $H[m, k] = 0$, $\forall |m-k| > 1$. This allows the separation of frequency-domain measurements into two sets, one for channel estimation and the other for data demodulation. Specifically, define the pilot index as

$$\{i_g\} = \{8g + 1\}, \quad g = -K/16, \ldots, K/16 - 1. \tag{29}$$

The left and right neighbors of pilot subcarriers (which are null-subcarriers) are indexed by $\{i_g^-\}$ and $\{i_g^+\}$, where $\{i_g^\pm\} = \{i_g \pm 1\}$. Define a $K \times K$ diagonal selector matrix $\mathbf{\Phi}$,

whose diagonal entry is one if the index belongs to $\{i_g^-, i_g, i_g^+\}$ and zero otherwise. As such, $\mathbf{\Phi z}$ contains the measurements related to channel estimation, while $\mathbf{z} - \mathbf{\Phi z}$ contains the measurements related to data demodulation.

This paper adopts the OMP algorithm[32] for sparse channel estimation. Define $\mathbf{z}_\mathrm{p} = \mathbf{\Phi z}$ as the measurement vector, and $\mathbf{v}_\mathrm{P}$ as the corresponding noise vector. Define $\mathbf{s}_\mathrm{P} = \mathbf{\Phi s}$ as the known pilot vector. The measurement model for channel estimation is

$$\begin{aligned}\mathbf{z}_\mathrm{P} &= \mathbf{H}\mathbf{s}_\mathrm{P} + \mathbf{v}_\mathrm{P} \\ &= \sum_{p=1}^{N_\mathrm{pa}} \sum_{n=0}^{N_\mathrm{amp}} \xi_p^{(n)} \Lambda_p \Gamma_p^{(n)} \mathbf{s}_\mathrm{P} + \mathbf{v}_\mathrm{P}. \end{aligned} \tag{30}$$

To use OMP for channel estimation, the receiver constructs a dictionary of signal templates parameterized by tentative assignments on possible parameters. This work assumes that the parameters (τ_p', b_p) fall on the following grids

$$\tau' \in \left\{0, \frac{T}{\lambda K}, \frac{2T}{\lambda K}, \ldots, T_g\right\}, \tag{31}$$

$$b \in \{-b_\mathrm{max}, -b_\mathrm{max} + \Delta b, \ldots, b_\mathrm{max}\}. \tag{32}$$

The grid on τ' is based on the assumption that after synchronization all arriving paths fall into an interval of length no larger than T_g, where the time resolution is chosen as a fraction $1/\lambda$ of the baseband sampling interval T/K, leading to $N_1 = \lambda K T_g / T$ tentative delays. The residual Doppler rates are assumed to spread around zero after compensation by resampling and CFO compensation. With b_max as the maximum Doppler value and Δb as the Doppler scale resolution, there are $2b_\mathrm{max}/(\Delta b) + 1 = N_2$ points on the Doppler scale grid. Overall, there are $N_1 N_2$ candidate paths defined on the two-dimensional delay-Doppler plane that will be searched. Although a large number of tentative paths are necessary to construct an accurate dictionary, most paths will have zero energy, and the problem is sparse.

By searching over $N_1 N_2$ tentative paths, the linear formulation of the problem in Eq. (30) is

$$\mathbf{z}_\mathrm{P} = \sum_{n=0}^{N_\mathrm{amp}} \sum_{p=1}^{N_1 N_2} \xi_p^{(n)} \mathbf{\Lambda}_p \mathbf{\Gamma}_p^{(n)} \mathbf{s}_\mathrm{P} + \mathbf{v}_\mathrm{P} = \mathbf{A}\boldsymbol{\xi} + \mathbf{v}_\mathrm{P}, \tag{33}$$

where

$$\mathbf{A} = [\mathbf{A}^{(0)}, \ldots, \mathbf{A}^{(n)}, \ldots, \mathbf{A}^{(N_\mathrm{amp})}], \tag{34}$$

$$\mathbf{A}^{(n)} = \left[\mathbf{\Lambda}_1 \mathbf{\Gamma}_1^{(n)} \mathbf{s}_\mathrm{P}, \cdots, \mathbf{\Lambda}_{N_1 N_2} \mathbf{\Gamma}_{N_1 N_2}^{(n)} \mathbf{s}_\mathrm{P}\right], \tag{35}$$

$$\boldsymbol{\xi} = \left[\xi_1, \ldots, \xi_{N_1 N_2}, \ldots, \xi_1^{(N_\mathrm{amp})}, \ldots, \xi_{N_1 N_2}^{(N_\mathrm{amp})}\right]^T. \tag{36}$$

The template matrix $\mathbf{A}$ has $N_\mathrm{amp} N_1 N_2$ columns, and most of the entries of $\boldsymbol{\xi}$ will be zeros. Identifying the significant paths one at a time, the OMP algorithm solves a constrained least-squares (LS) problem at each iteration to measure the fitting error.[32] The residual fitting error is compared with a threshold based on the noise power to determine the termination of the algorithm. In our implementation, we first identify the paths using the templates in $\mathbf{A}^{(0)}$, and then search for additional $\{\xi_p^{(n)}\}_{n=1}^{N_\mathrm{amp}}$ only on those (delay, Doppler) points already identified.

The complexity of the channel estimation based on OMP is decided by the size of the dictionary. If a first-order polynomial fitting is used on delay, the dictionary size is $N_\mathrm{amp} N_1 N_2$. If a zeroth-order polynomial fitting is used on delay, i.e., $b_p = 0$, the dictionary size reduces to $N_\mathrm{amp} N_1$. The dictionary size grows only linearly with the order of the polynomial on amplitude, but multiplicatively on the order of the polynomial on delay.

Data demodulation is applied on each group separately. For the gth group with three data symbols $s[i_g + 4]$, $s[i_g + 5]$, $s[i_g + 6]$, the related measurements are $z[i_g + 3]$, $z[i_g + 4]$, $z[i_g + 5]$, $z[i_g + 6]$, $z[i_g + 7]$. A linear minimum-mean-square-error (MMSE) equalizer is adopted,[28,29] where the noise variance is estimated based on the energy on the null subcarriers. The symbol estimates at the MMSE equalizer output are passed to the nonbinary LDPC decoder.[31] The block error rate (BLER), defined as the ratio of the number of OFDM blocks with decoding errors to the total number of OFDM blocks received, is used as the performance metric.

C. Experimental results: SPACE08

The signal sets were transmitted during SPACE08, which was held off the coast of Martha's Vineyard, MA, during October 2008. The water depth was about 15 m. The transmitter was about 4 m above the sea floor, while the receiver arrays were about 3.25 m above the sea floor. In this scenario, resampling is not necessary because the transmitter and the receiver arrays were stationary, i.e., $\hat{a} = 0$. The residual Doppler shift compensation is carried out to minimize the energy on the null subcarriers.[19]

In general, using high-order polynomials in the proposed channel parameterization reduces the model mismatch, but increases the number of unknowns to be estimated. The polynomial order is difficult to decide *a*

TABLE I. Different configurations of polynomial orders.

Different cases	(0,0)	(1,0)	(2,0)	(0,1)	(1,1)	(2,1)
Amplitude polynomial-fitting order	0	1	2	0	1	2
Delay polynomial-fitting order	0	0	0	1	1	1
Number of unknown path-specific parameters	$2N_\mathrm{pa}$	$3N_\mathrm{pa}$	$4N_\mathrm{pa}$	$3N_\mathrm{pa}$	$4N_\mathrm{pa}$	$5N_\mathrm{pa}$
OMP dictionary size	N_1	$2N_1$	$3N_1$	$N_1 N_2$	$2N_1 N_2$	$3N_1 N_2$

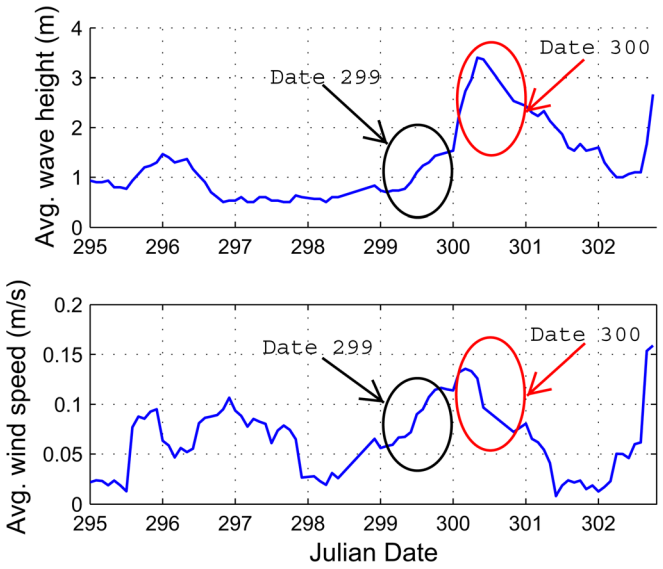

FIG. 2. (Color online) The average wave height for selected days of the SPACE08 experiment. Bottom: The average wind speed for the same range of days.

priori. We tested six specific cases, with zeroth-order or first-order fitting on delay variation together with zeroth-order, first-order, or second-order fitting on amplitude variation; we reiterate that although the polynomial on the delay is up to the first order, the polynomial on the amplitude is not limited to the second order tested here. These six cases are listed in Table I. For the OMP algorithm, the complexity is proportional to the dictionary size. In our tests, the number of grid points along the delay and Doppler dimensions are 480 and 15, respectively, i.e., $N_1 = 480$ and $N_2 = 15$.

The average wave height and wind speed were recorded during the experiment, as shown in Fig. 2. On each day, one data burst (containing 20 OFDM blocks in the format as described in Sec. IV A, and OFDM blocks in other formats) was transmitted once every 2 h. We choose the data sets

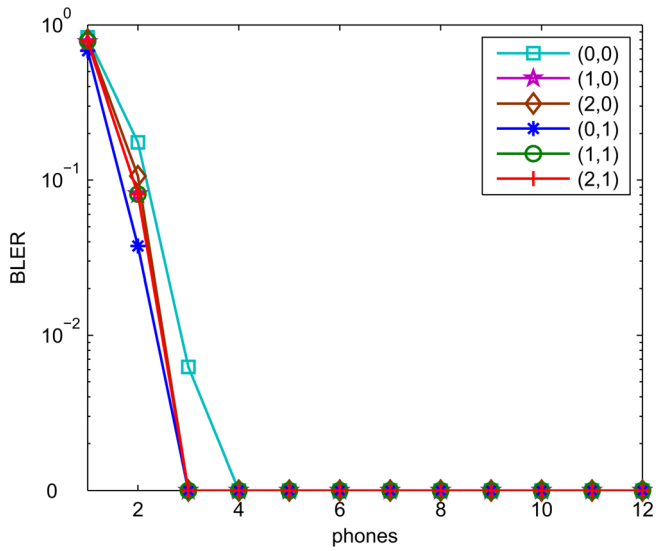

FIG. 3. (Color online) The decoding results with data collected in Julian date 299, receiver S1, 16-QAM. The legend (*a, b*) means that an *a*th-order polynomial is used to parameterize amplitude variation and a *b*th-order polynomial is used to parameterize the delay variation.

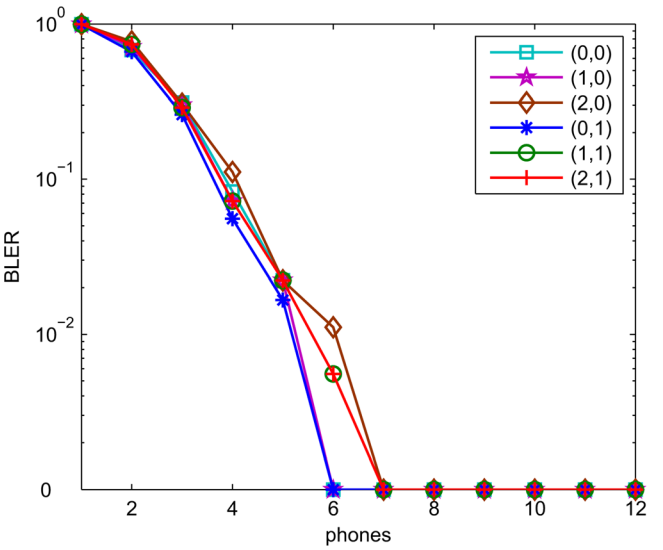

FIG. 4. (Color online) The decoding results with data collected in Julian date 299, receiver S3, 16-QAM.

from two days to verify the receiver performance. Figure 2 suggests that Julian date 300 is the most challenging day due to large wave height and wind speed. This intuitive reasoning is confirmed by the published performance results.[28] Here we consider two consecutive days, and view Julian date 299 as one calm day and Julian date 300 as one challenging day. The receivers with six different approximations on the multipath channel are used to decode these data sets.

1. Performance with slowly-varying channels

Figures 3 and 4 show the BLER performance for Julian date 299 at receivers S1 (60 m away from the transmitter) and S3 (200 m away), respectively. All six cases have almost the same performance. This means that it is not necessary to choose high polynomial orders to characterize these type of channels. Because the low-order polynomial fitting leads to low complexity and requires small pilot overhead, the

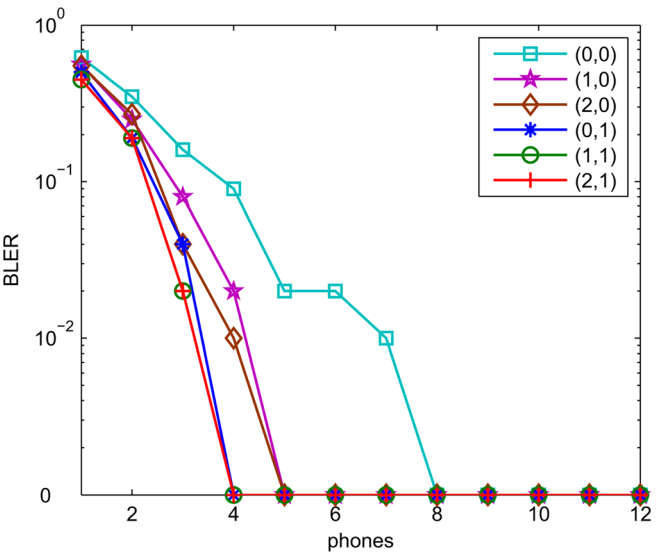

FIG. 5. (Color online) The decoding results with data collected in Julian date 300, receiver S1, 16-QAM.

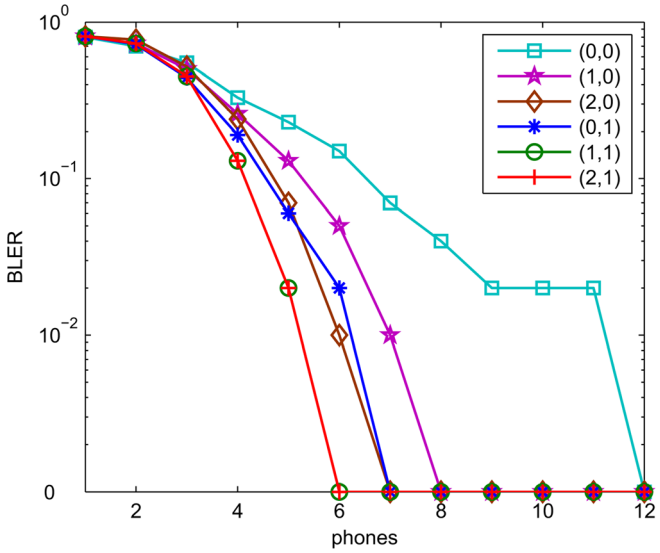

FIG. 6. (Color online) The decoding results with data collected in Julian date 300, receiver S3, 16-QAM.

parameterization used with small polynomial orders is suitable when the channels are varying slowly.

2. Performance with quickly-varying channels

Figures 5 and 6 show the BLER performance for Julian date 300, where different cases have quite different BLER performance. The following observations are in order.

(1) The channels are quickly-varying, since the (0,0) configuration has much worse performance than all other configurations.
(2) With the same amplitude polynomial-fitting order, the performance with first-order delay fitting is better than that of the zero-order fitting. The performance is improved at the cost of implementation complexity.
(3) The performance of the (0,1) configuration is better than that of (1,0), but similar to that of the (2,0) configuration. Since the (2,0) configuration entails lower channel estimation complexity, it offers an interesting alternative to the (0,1) configuration, while the latter has been extensively used in the literature.[5,19]
(4) The performance with the (1,1) configuration is better than that of the (0,1) configuration, indicating that it is still worthwhile to incorporate amplitude variation even after approximating the delay variation. The performance of the (2,1) configuration is similar to that of the (1,1) configuration, indicating that there is no need to increase the fitting order any more for this data set.

The results in Figs. 5 and 6 provide evidence that further incorporating the amplitude variation in addition to the path delay variation can help to enhance the receiver performance in the presence of quickly-varying channels.

V. CONCLUSIONS

This paper proposed to parameterize both path amplitude and delay variations for UWA multipath channels. With one polynomial to approximate the amplitude variation and one polynomial up to the first order to approximate the delay variation for each path, the exact discrete-time channel input–output relationship tailored for zero-padded OFDM was derived. The benefits of exploring both path amplitude and delay variations was shown by one signal design with data sets collected from the SPACE08 experiment. Also, high-order fitting on the amplitude with zero-order fitting on the delay is one interesting alternative to the currently used approach of zero-order fitting on the amplitude and first-order fitting on the delay.

Apparently, in calm environments, low-order polynomials can be used, while high-order polynomials help to improve the system performance in more dynamic conditions. One key practical issue that warrants further study is how to select the polynomial fitting orders for online receiver processing. One could use the knowledge on the environmental parameters to assist the selection of the polynomial orders. For this, one would need to establish connections between the channel parameterization approach from a pure signal processing point of view and the physics-based channel modeling approaches.[15–17] Or, considering slow channel variations, one can use the performance results from the previous blocks to decide the polynomial orders for the current block. Another approach is to increase the fitting orders on amplitude and delay gradually on the fly without any prior knowledge, following the progressive receiver concept.[33] These choices need to be compared, using experimental data collected from different environments.

ACKNOWLEDGMENTS

This work is supported by the ONR Grant No. N00014-09-1-0704. We thank Dr. James C. Preisig and his team for conducting the SPACE08 experiment. We thank the reviewers for the comments that have helped to improve the presentation of this paper.

[1]D. B. Kilfoyle and A. B. Baggeroer, "The state of the art in underwater acoustic telemetry," IEEE J. Ocean. Eng. **25**, 4–27 (2000).
[2]M. Stojanovic and J. Preisig, "Underwater acoustic communication channels: Propagation models and statistical characterization," IEEE Commun. Mag. **47**, 84–89 (2009).
[3]M. Stojanovic, J. A. Catipovic, and J. G. Proakis, "Phase-coherent digital communications for underwater acoustic channels," IEEE J. Ocean. Eng. **19**, 100–111 (1994).
[4]W. Li and J. C. Preisig, "Estimation of rapidly time-varying sparse channels," IEEE J. Ocean. Eng. **32**, 927–939 (2007).
[5]C. R. Berger, S. Zhou, J. Preisig, and P. Willett, "Sparse channel estimation for multicarrier underwater acoustic communication: From subspace methods to compressed sensing," IEEE Trans. Signal Process. **58**, 1708–1721 (2010).
[6]K. Tu, D. Fertonani, T. M. Duman, M. Stojanovic, and J. G. P. P. Hursky, "Mitigation of intercarrier interference for OFDM over time-varying underwater acoustic channels," IEEE J. Ocean. Eng. **36**, 156–171 (2011).
[7]J. G. Proakis, *Digital Communications*, 4th ed. (McGraw-Hill, New York, 2001), Chap. 14.
[8]T. Zemen and C. F. Mecklenbrauker, "Time-variant channel estimation using discrete prolate spheroidal sequences," IEEE Trans. Signal Process. **53**, 3597–3607 (2005).
[9]G. B. Giannakis and C. Tepedelenlioglŭ, "Basis expansion models and diversity techniques for blind identification and equalization of time-varying channels," Proc. IEEE **86**, 1969–1986 (1998).

[10]X. Ma, G. B. Giannakis, and S. Ohno, "Optimal training for block transmissions over doubly-selective wireless fading channels," IEEE Trans. Signal Process. **51**, 1351–1366 (2003).
[11]I. Cha and S. A. Kassam, "Channel equalization using adaptive complex radial basis function networks," IEEE J. Sel. Areas Commun. **52**, 48–59 (2003).
[12]X. Zhou and X. Wang, "Channel estimation for OFDM systems using adaptive radial basis function networks," IEEE Trans. Veh. Technol. **25**, 4–27 (2000).
[13]M. I. Lee, S. K. Oh, and M. H. Sunwoo, "An improved channel estimation scheme using polynomial-fitting and its weighted extension for an MC-CDMA/TDD uplink system with pre-equalization," in *Proceedings of Vehicular Technology Conference* (2004), pp. 419–423.
[14]D. K. Borah and B. D. Hart, "Frequency-selective fading channel estimation with a polynomial time-varying channel model," IEEE Trans. Commun. **47**, 862–873 (1999).
[15]P. H. Dahl, "On bistatic sea surface scattering: Field measurements and modeling," J. Acoust. Soc. Am. **105**, 2155–2169 (1999).
[16]F. Tappert, "The parabolic approximation method," in *Wave Propagation and Underwater Acoustics*, edited by J. Keller and J. Papadakis (Springer, Berlin, 1977), pp. 224–287.
[17]A. Song, J. Senne, M. Badiey, and K. Smith, "Underwater acoustic communication channel simulation using parabolic equation," in *Proceedings of the ACM International Workshop on UnderWater Networks (WUWNet)*, Seattle, WA (2011), pp. 1–5.
[18]A. Song, M. Badiey, A. Newhall, J. F. Lynch, H. A. DeFerrari, and B. G. Katsnelson, "Passive time reversal acoustic communications through shallow water internal waves," IEEE J. Ocean. Eng. **35**, 756–764 (2010).
[19]B. Li, S. Zhou, M. Stojanovic, L. Freitag, and P. Willett, "Multicarrier communication over underwater acoustic channels with nonuniform Doppler shifts," IEEE J. Ocean. Eng. **33**, 198–209 (2008).
[20]M. Stojanovic, "Low complexity OFDM detector for underwater channels," in *Proceedings of MTS/IEEE OCEANS Conference*, Boston, MA (2006), pp. 1–6.
[21]T. Kang and R. Iltis, "Iterative carrier frequency offset and channel estimation for underwater acoustic OFDM systems," IEEE J. Sel. Areas Commun. **26**, 1650–1661 (2008).
[22]T. Kang, H. C. Song, W. S. Hodgkiss, and J. S. Kim, "Long-range multicarrier acoustic communications in shallow water based on iterative sparse channel estimation," J. Acoust. Soc. Am. **128**, EL372–EL377 (2010).
[23]J. Zhang and Y. R. Zheng, "Bandwidth-efficient frequency-domain equalization for single carrier multiple-input multiple-output underwater acoustic communications," J. Acoust. Soc. Am. **128**, 2910–2919 (2010).
[24]J. Tao, Y. R. Zheng, C. Xiao, and T. C. Yang, "Robust MIMO underwater acoustic communications using turbo block decision-feedback equalization," IEEE J. Ocean. Eng. **35**, 948–960 (2010).
[25]F. Qu and L. Yang, "Basis expansion model for underwater acoustic channels?," in *Proceedings of MTS/IEEE OCEANS Conference*, Quebec City, Canada (2008), pp. 1–7.
[26]G. Leus and P. van Walree, "Multiband OFDM for covert acoustic communications," IEEE J. Sel. Areas Commun. **26**, 1662–1673 (2008).
[27]S. Hwang and P. Schniter, "Efficient multicarrier communication for highly spread underwater acoustic channels," IEEE J. Sel. Areas Commun. **26**, 1674–1683 (2008).
[28]S. Mason, C. Berger, S. Zhou, K. Ball, L. Freitag, and P. Willett, "Receiver comparisons on an OFDM design for Doppler spread channels," in *Proceedings of MTS/IEEE OCEANS Conference*, Bremen, Germany (2009), pp. 1–7.
[29]S. Mason, C. Berger, S. Zhou, K. Ball, L. Freitag, and P. Willett, "An OFDM design for underwater acoustic channels with Doppler spread," in *Proceedings of the 13th DSP Workshop*, Marco Island, FL (2009), pp. 138–143.
[30]S. Mason, C. R. Berger, S. Zhou, and P. Willett, "Detection, synchronization, and Doppler scale estimation with multicarrier waveforms in underwater acoustic communication," IEEE J. Sel. Areas Commun. **26**, 1638–1649 (2008).
[31]J. Huang, S. Zhou, and P. Willett, "Nonbinary LDPC coding for multicarrier underwater acoustic communication," IEEE J. Sel. Areas Commun. **26**, 1684–1696 (2008).
[32]J. A. Tropp and A. C. Gilbert, "Signal recovery from random measurements via orthogonal matching pursuit," IEEE Trans. Inf. Theory **53**, 4655–4666 (2007).
[33]J.-Z. Huang, S. Zhou, J. Huang, C. Berger, and P. Willett, "Progressive inter-carrier interference equalization for OFDM transmission over time-varying underwater acoustic channels," IEEE J. Sel. Top. Signal Process. **5**, 1524–1536 (2011).